R.E.M. (Rekayasa Energi Manufaktur) Jurnal / Vol.5 no.2/2020 / ISSN online (2528-3723)

Effect Of Preheating On The Hardness And Microstructure In Shielded Metal Arc Weldments Of A283 B

Ali Akbar
Teknik Mesin Universitas Muhammadiyah Sidoarjo, Jl. Raya Gelam No.250 Sidoarjo
Email: aliakbar@umsida.ac.id

Abstract. *The purpose of this study was to determine the effect of heating on the welding process of SMAW (Shielded Metal Arc Welding) in terms of hardness and microstructure of welded metal. Much welding has been done by preheating but below the temperature used below the initial martensitic temperature which reaches 452 ° C, this data is sourced from research by S.Zheng et.al and Y. Huang et.al. For this reason, an experiment was carried out with heat temperatures above a martensitic temperature of 500 ° C. The results show that in the Weld Metal area the pearlite structure appears larger, the effect of current strength on HAZ width is directly proportional, the greater the current strength, the wider HAZ, and hardness are affected by the rough grains of martensite*

Keywords- *Microstructure, HAZ Width, Hardness, Preheat, Pearlite, Ferrite*

How to cite: Ali Akbar[1] ,Mulyadi[2], N.H.Wiyono[3] (2020) Effect Of Preheating On The Hardness And Microstructure In Shielded Metal Arc Weldments Of A283 B. R.E.M. (Rekayasa Energi Manufaktur) Jurnal 5 (2) *doi: 10.21070/rem.v5i2.1279*

INTRODUCTION

One welding technique that is widely used for joining steel construction is the welding process of SMAW (Shielded Metal Arc Welding). SMAW is commonly used in industry because it uses low-cost electrodes and can be easily carried out compared to other welding techniques [1, 2]. All arc welding processes use a high-temperature heat source, the temperature difference occurs between the area that is heating due to the arc with the cold parent metal [3]. Temperature differences cause differences in thermal expansion. Contractions and high stress, these things can be minimized by reducing the temperature difference by heating up at the beginning of the welding process.

P. K. Ghosh et al. [4] studied the effect of heat treatment before and after welding on the mechanical properties and microstructure of 9Cr-1Mo (V-Nb) steel pipe joints modified in the SMAW and TIG welding processes. They reported that heat treatment before and after welding significantly affected the microstructure of the welding area and HAZ in both welding processes. P. Deb et al. [5] studied the connection characteristics of HY-80 SMAW steel that had been heated and not heated using a transmission electron microscope and concluded that the welding that was heated had more hardness than that which was not heated.

J. O. Olawale et al. [6] studied the correlation between various SMAW parameters and post welding heat treatment on low carbon steel. They reported that with an increase in welding current, the hardness and ultimate tensile strength (UTS) increased but there was a decrease in impact strength. The impact strength increases while hardness and UTS decrease at normal temperature increases. A. M. Tahir et al. [7] studied the mechanical properties of AISI 1020 low carbon steel joints welded by SMAW using different electrodes and current values. They report that mechanical properties such as hardness and tensile strength decrease with increasing heat input.

A. Gupta et al. [8] studied the effects of heat input on the microstructure and corrosion behavior of the super duplex steel UNS S32750 using scanning and optical electron microscopy at SMAW. They concluded that welding behavior is influenced by heat input. Munawar et al. [9] studied the effect of SMAW on the mechanical properties of S45c steel with and without heat treatment.

http://doi.org/10.21070/rem.v5i2.1279

They report that higher temperatures result in increased material strength and mechanical properties change when heated at temperatures of 150 C, 250 C, and 300 C.

Weiwei Yu et al. [10] compared the SMAW and GTAW welding of Z3CN20.09M primary cooling pipes based on the toughness of their fractures on the base metal, weld metal, HAZ and fusion zones. They reported that weld metal was wider in SMAW welding with a more asymmetrical distribution of microhardness than in GTAW welds. The effect of this thermal cycle is very large on the weld finish because it determines the structure and mechanical properties of the workpiece. This study aims to determine the effect of heating on the SMAW welding process in terms of hardness and microstructure of welded metal.

MATERIALS AND METHODS

Material used and electroda specifications

The specimen used in this study was A283 B low carbon steel plate which has a chemical composition in table 2.1. While the electrodes used in this study have their own chemical composition in Table 2.2.

Table 2.1 *Chemical composition of steel A283 B*

Material	Chemical Composition				
A283 B	C	Mn	P	S	N
	0,21% Max	1,50%	0,045%	0,045%	0,009%

Table 2.2 *Chemical Composition of the LB-52 AWS E7016 and RB-26 AWS E6013 Electrodes*

Brand	Si%	Mn%	C%	P%	S%
LB-52 AWS E7016	0,60	0,94	0,08	0,011	0,006
RB-26 AWS E6013	0,08	0,30	0,37	0,012	0,010

Welding process

Before the welding process, a specimen of material A283 B 8mm thick is cut with a size (100x200) mm. Then formed seam V with an angle of 90º depth of 6mm, gap (2x2) mm. Welding is carried out in a flat position with variations in the welding current shown in table 2.3. Before the welding process is carried out the specimen is heated first with temperatures reaching 500ºC. The heating is done using a blander whose gas is in the form of oxy-acetylene, then welding is carried out by maintaining the preheat temperature by using a digital thermometer. The results of the welding process are shown in Figure 2.1.

Table 2.3 *Welding variations*

Specimen	LB-52 AWS E7016	Specimen	RB-26 AWS E6013
A1	130	B1	130
A2	140	B2	140
A3	150	B3	150
A4	160	B4	160

Figure 2.1 *The results of the welding process before testing*

http://doi.org/10.21070/rem.v5i2.1279

Testing process

Macro Etching Process and Micro Structure

The etching macro test is used to obtain the macrostructure of the workpiece, namely four welding areas (Weld Metal, Fusion Line, HAZ and Base Metal). The etching macro is done by polishing the specimen with sandpaper up to 1000 grids and then etching until the weld area is visible [11]. After macro etching testing then proceeds with microstructure testing.

The procedures for preparation and implementation of the test are as follows:

1. Before conducting the macro etching test, polishing is done using Silicon Carbide scouring paper from grid 80 to grid 2000. After that, the macro etching is done using a 1-2% HNO3 solution in 97% alcohol solution. With a dipping time of 1.5 - 2 seconds.
2. After dipping, the specimen is cleaned with water and dried to see etching results.
3. After the expected results are obtained, the width of the HAZ formed is calculated. How to measure the HAZ width by using a measuring instrument such as the ruler, which is measured is the width of the area between the fusion line and the base metal.
4. Then the process of taking the results of microstructure using a microscope.

Hardness Testing Process.

After obtaining a microstructure image, a hardness test is then performed with the following procedure:

1. Specimens from microstructure testing are marked as indentations.
2. The indentation place is located on the weld metal, HAZ is near weld metal, HAZ is near the base metal
3. Testing is carried out with a Rockwell hardness testing machine.

RESULTS

Micro Etching Test Results

Microstructure observation is carried out to determine the grain size in the area (1) Base Metal, (2) HAZ and (3) Welding Metal, so that changes and phenomena can occur in the results of welding. In Figure 3.1 the LB-52 AWS E7016 welding electrode heats initial 500ºC, the microstructure in the Base Metal region is dominated by ferrite structures that appear whiter in color relative to each current variation. Whereas in the Weld Metal area the pearlite structure appears larger because there are 2 phases formed by customization, with the composition of the eutectoid being transformed into ferrite and carbide. This is because ferrite and carbide are formed together and the exit is mixed with one another. If the rate of cooling is done slowly then the carbon atom can diffuse longer and can travel longer distances, so that it gets a large pearlite shape proportional to the magnitude of the strong current. And, whereas in the HAZ region the ferrite microstructure is also still dominant compared to the pearlite structure. Where the E7016 electrode contains low hydrogen less than 0.5% so that the welding deposit can be free of porosity.

In Figure 3.2 welding of the RB-26 AWS E6013 preheat 500ºC electrode, the microstructure in the Base Metal region is dominated by a ferrite structure that appears to be more white in color relative to each current variation. Whereas in the Weld Metal area the pearlite structure appears larger because there are 2 phases formed austenitic, with the composition of the eutectoid transformed into ferrite and carbide. This is because ferrite and carbide are formed simultaneously and the exit mixes with each other. If the cooling rate is carried out slowly then the carbon atom can diffuse longer and can travel longer distances, so that a large pearlite shape is obtained with increasing currents, whereas in the HAZ region the ferrite microstructure is also still large compared to the pearlite structure as the current increases. Where this E6013 electrode contains more potassium makes it easy to use at low engine voltage.

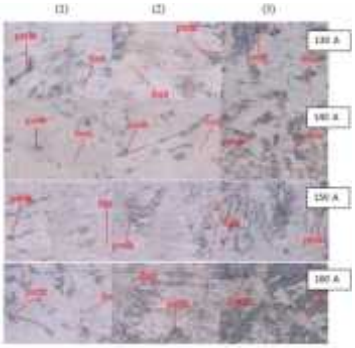

Figure 3.1 *Microstructure of specimen A welding using LB-52 AWS E7016 electrodes with a magnification of 500x*

http://doi.org/10.21070/rem.v5i2.1279

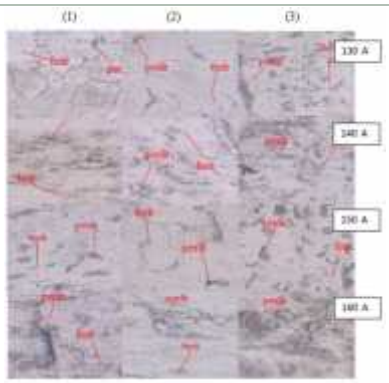

Figure 3.2 *Microstructure of Specimen B Welding Using RB-26 AWS E6013 Electrodes*

Macro Etching Test Results

Macro observations on weld results were carried out to determine the shape and width of the HAZ (Heat Effected Zone) area. The results of observations in macro testing of specimens as in Figure 3.3 and 3.4 below

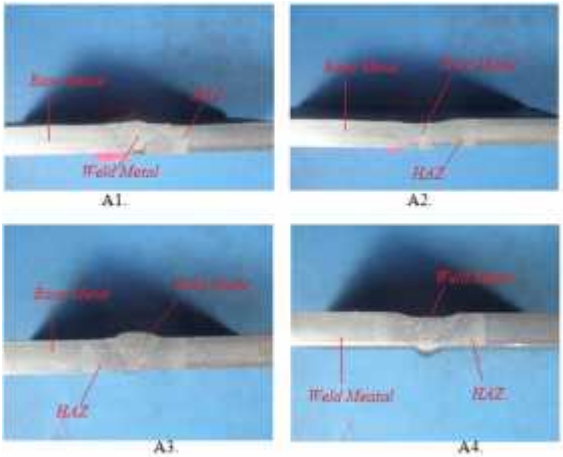

Figure 3.3 *Photo Macro Electrodes LB-52 AWS E7016 Current A1. 130A, A2. 140 A, A3. 150A, and A4. 160A*.

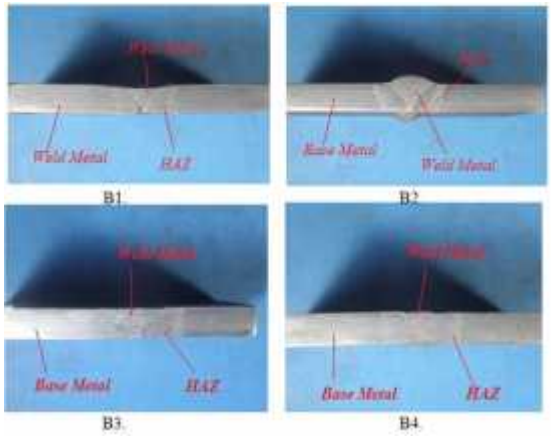

Figure 3.4 *Macro Photo Electrode Rb 26 AWS E6013rus B1. 130A, B2.140 A, B3. 150A, and B4. 160A*

Macro observations on welding results are not only used to determine the shape and width of the HAZ but also to observe the depth of weld penetration. The shape and width of the HAZ are basically influenced by the heat input and welding speed. The results of the measurement of the HAZ width of each current and electrode variation are found in table 3.1. In specimen A and specimen B, each HAZ width increases proportionally to the increase in current strength used.

http://doi.org/10.21070/rem.v5i2.1279

Table 3.1 *Comparison of Non Preheat and Preheat HAZ Width of 500ºC*

No. Specimen	Current	HAZ width Non-Preheat	HAZ width Preheat 500ºC
A1	130 A	3,6 mm	5,8 mm
A2	140 A	4,55 mm	6,4 mm
A3	150 A	5,26 mm	6,9 mm
A4	160 A	5,7 mm	7,7 mm
B1	130 A	3,6 mm	5,5 mm
B2	140 A	4,25 mm	6 mm
B3	150 A	5 mm	6,6 mm
B4	160 A	5,5 mm	7,3 mm

Results of Hardness Testing

Vickers hardness test with HV 10, as for the hardness testing points measured in each welding area (Base Metal, HAZ, and Weld Metal) there are three points as in Figure 3.5 below:

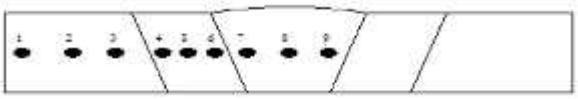

Figure 3.5 *Position of the test point*

Data of welding hardness distribution values using Lb 52 AWS E7016 electrodes and Rb AWS E6013 using different currents, where point 1,2,3 is the Base Metal region, point 4,5,6 is the HAZ region, and point 7,8, 9 is a Weld Metal area. Where the hardness value of each specimen is entered in tables 3.2 and 3.3 below:

Table 3.2 *Vickers hardness test results using LB-52 AWS E7016 electrodes*

Point	Regional	Specimen			
		130A	140A	150A	160A
1	Base Metal	106,7	108,4	110	119,5
2		107,5	109,3	110,5	120,2
3		108,3	109,5	120,2	123
4	HAZ	113,7	121,3	120	130
5		115	122,4	120,9	130,2
6		116,8	122,8	122,1	130,8
7	Weld Metal	173	174,1	173,5	179
8		173	174,7	176,9	187,3
9		170	173,8	177,3	187

Table 3.3 *Vickers hardness test results using RB-26 AWS E6013 electrodes*

Titik	Daerah	Spesimen			
		130A	140A	150A	160A
1	Base Metal	106,6	107,2	110	119,3
2		107,3	108,1	110,5	120
3		108	108,4	110,9	120,7
4	HAZ	111,9	118	119	122
5		113,1	121,1	120,4	122,3
6		115,7	122,6	120,7	122,5
7	Weld Metal	168	169,2	173	177,2
8		173	173,7	176	185
9		170	173,5	173,3	177

http://doi.org/10.21070/rem.v5i2.1279

In Figure 3.6 the maximum value of the hardness test results is at point 8 of this welding process results using LB-52 AWS E7016 electrodes, while in Figure 3.7 the maximum value of the hardness test results is at point 8 of the results of the welding process using RB-26 AWS E6013 electrodes. The effect of heat on the weld metal greatly determines the hardness of the welding process

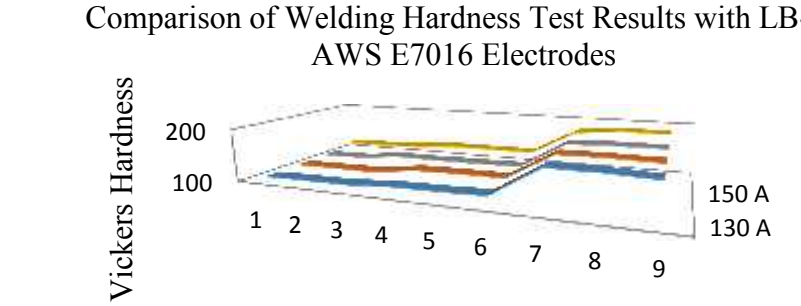

	1	2	3	4	5	6	7	8	9
130 A	106.7	107.5	108.3	113.7	115	116.8	173	173	170
140 A	108.4	109.3	109.5	121.3	122.4	122.8	174.1	174.7	173.8
150 A	110	110.5	120.2	120	120.9	122.1	173.5	176.9	177.3
160 A	119.5	120.2	123	130	130.2	130.8	179	187.3	187

Figure 3.6 *Test results of specimen hardness A*

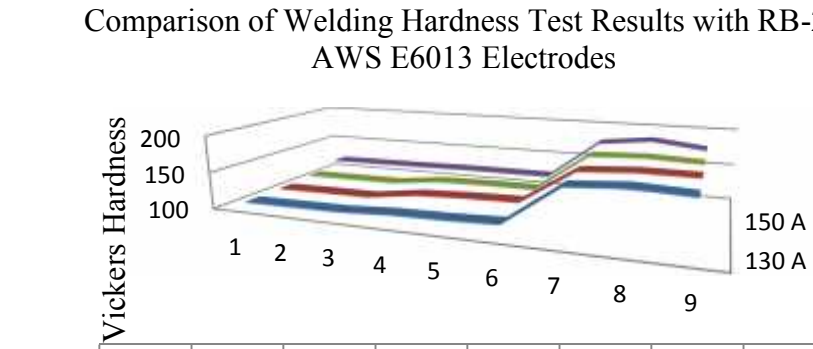

	1	2	3	4	5	6	7	8	9
130 A	106.6	107.3	108	111.9	113.1	115.7	168	173	170
140 A	107.2	108.1	108.4	118	121.1	122.6	169.2	173.7	173.5
150 A	110	110.5	110.9	119	120.4	120.7	173	176	173.3
160 A	119.3	120	120.7	122	122.3	122.5	177.2	185	177

Figure 3.7 *Specimen hardness test results B*

DISCUSSION

Pearlite transformations can occur at the austenitic grain boundaries or at homogeneity such as inclusions [12]. At high transformation temperatures, pearlite forms nodules from alternative ferrite and cementite lamella which may be quite rough [13]. The experimental results in the Weld Metal region of pearlite structure appear larger because there are 2 phases formed austenite, with eutectoid composition transformed into ferrite and carbide. The reasons for the tendency for maximum HAZ hardness can be explained as follows, the preheating function before welding is the same as slowing down the cooling rate, and hardness is contributed by the microstructure and grain size. According to reference. [14,15], the initial temperature of martensite is 452 ° C. When the to preheat temperature is below 500 ° C, the rapid cooling rate and more martensitic remain.

http://doi.org/10.21070/rem.v5i2.1279

Then the violence was mainly contributed by coarse grains and martensite. While preheat temperatures are higher than 500 ° C, which is more than the initial temperature of martensite, the rate of martensitic transformation is fast and the amount of martensite decreases and results in a decrease in hardness.

CONCLUSIONS

The results of the effect of preheating on the hardness and microstructure of the welding material of SM28 A283 B are summarized as follows:

The results of experiments in the Weld Metal area of pearlite structures appear larger because there are 2 phases of formed austenite, with the composition of the eutectoid being transformed into ferrite and carbide.

The effect of current strength on the width of the HAZ is proportional to the greater strength of the wider HAZ current.

Violence is affected by coarse grains and martensite. While the preheating temperature is higher than 500 ° C, which is more than the initial temperature of martensite, the rate of martensitic transformation is fast and the amount of martensite decreases and results in a decrease in hardness

ACKNOWLEDGMENTS

The author would like to thank all the support given to complete this research which we cannot mention one by one. In particular, we thank Nur Hadi Wiyono for contributing to the data collection for this research.

REFERENCES

[1] Buchely MF, Gutierrez JC, Leon LM, Toro A. The effect of microstructure on abrasive wear of hardfacing alloys. Wear 2005;259:52–61.

[2] Iswanto et al., Effect of Welding Using Electrodes With Certain Treatment on Stainless Steel 304 Using SMAW Welding, Covenant Journal of Engineering Technology, vol. 4, no. 2, pp. 50-55, 2020.

[3] Iswanto, Noerdianto, A'rasy Fachruddin dan Mulyadi, Analisa Perbandingan Kekuatan Hasil Pengelasan TIG dan Pengelasan MIG pada Aluminium 5083, Jurnal Turbo, vol. 9, no. 1, pp. 87-92, 2020.
DOI: http://dx.doi.org/10.24127/trb.v9i1.1166

[4] P.K. Ghosh, U. Singh, Influence of pre- and post-weld heating on weldability of modified 9Cr–1Mo(V–Nb) steel pipe under shielded metal arc and tungsten inert gas welding processes, Sci. Technol. Weld. Joining 9 (3) (2004) 229–236.

[5] P. Deb, K.D. Challenger, D.R. Clark, Transmission electron microscopy characterizations of preheated and non-preheated shielded metal arc weldments of HY-80 steel, Mater. Sci. Eng. 77 (1986) 155–167.

[6] J.O. Olawale, S.A. Ibitoye, K.M. Oluwasegun, M.D. Shittu, R.C. Ofoezie, Correlation between process variables in shielded metal arc welding (SMAW) process and post weld heat treatment (PWHT) on some mechanical properties of low carbon steel welds, J. Min. Mater. Charact. Eng. 11 (2012) 891–895.

[7] Abdullah Mohd Tahir, Noor Ajian Mohd Lair, Foo Jun Wei, Investigation on mechanical properties of welded material under different types of welding filler (Shielded Metal Arc Welding), in: AIP Conference Proceedings-3rd International Conference on the Science and Engineering of Materials (ICoSEM 2017), 2018.

[8] Aman Gupta, Amit Kumar, T. Baskaran, Shashi Bhushan Arya, Rajesh Kisni Khatirkar, Effect of heat input on microstructure and corrosion behaviour of duplex stainless-steel shielded metal arc welds, Trans. Indian Inst. Metals 77 (7) (2018) 1595–1606.

[9] Munawar, Hammada Abbas, Ahmad Yusran Aminy, The effects of shielded metal arc welding (smaw) welding on the mechanical characteristics with heating treatment in S45c steel, J. Phys.: Conf. Series 962 (1) (2018.

[10] Yu. Weiwei, Minyu Fan, Jinhua Shi, Xu. Fei Xue, Hui Liu Chen, A comparison between fracture toughness at different locations of SMAW and GTAW welded joints of primary coolant piping, Eng. Fract. Mech. 202 (2018) 135–146.

[11] Iswanto, Edi Widodo, Ali Akbar dan Angga Kharisma Putra, Perbandingan Induction Hardening dengan Flame Hardening pada Sifat Fisik Baja ST 60, Mekanika, vol. 19, no. 2, 2020. DOI: https://doi.org/10.20961/mekanika.v19i2.43203

[12] H.K.D.H. Bhadeshia, R.W.K. Honeycombe, Steels Microstructure and Properties, Butterworth-Heinemann, 2011

[13] G. Thewlis, Classifcation and quantification of microstructures in steels, Mater. Sci. Technol. 20 (2004) 143–160.

[14] S. Zheng, Q. Wu, Q. Huang, et al., Influence of di□erent cooling rates on the mi- crostructure of the HAZ and welding CCT diagram of CLAM steel, Fusion Eng. Des. 86 (2011) 2616–2619.
[15] Y. Huang, X. Chen, Z. Shen, et al., Measurement and analysis of SHCCT diagram for CLAM steel, J. Nucl. Mater. 432 (s1-3) (2013) 460–465.

Conflict of Interest Statement:
The author declares that the research was conducted in the absence of any commercial or financial relationships that could be construed as a potential conflict of interest.

Article History:

Received: 25 Oktober 2020 | Accepted: 27 November 2020 | Published: 30 Desember 2020

http://doi.org/10.21070/rem.v5i2.1279